Single-crystal study of highly anisotropic CeNiGe$_2$

# Single-crystal study of highly anisotropic CeNiGe$_2$

## A P Pikul[1], D Kaczorowski, Z Bukowski, T Plackowski and K Gofryk

Institute of Low Temperature and Structure Research, Polish Academy of Sciences,
PO Box 1410, 50-950 Wrocław, Poland

E-mail: A.Pikul@int.pan.wroc.pl

## Abstract
High quality single crystals of CeNiGe$_2$ have been investigated by means of
magnetic susceptibility, magnetization, electrical resistivity, magnetoresistivity
and thermoelectric power measurements, carried out along all three principal
crystallographic directions. The compound is an antiferromagnetic Kondo
system that orders magnetically at $T_N = 3.9$ K and undergoes a spin structure
rearrangement at $T_1 = 3.2$ K. The magnetic behaviour is strongly anisotropic
with the easy magnetic direction parallel to the crystallographic $a$-axis. The
Kondo temperature and the total crystal field splitting are of the order of 20 and
100 K, respectively.

## 1. Introduction

CeNiGe$_2$ crystallizes in the orthorhombic CeNiSi$_2$-type structure (space group *Cmcm*, lattice
parameters: $a = 4.244(2)$ Å, $b = 16.747(10)$ Å, $c = 4.199(2)$ Å) [1]. Investigations
performed on polycrystalline samples have shown that the compound is a dense Kondo
system with an electronic specific heat coefficient $\gamma$ of about 220 mJ mol$^{-1}$ K$^{-2}$, ordering
antiferromagnetically at $T_N = 3.9$ K and undergoing another phase transition at $T_1 =
3.2$ K [2, 3]. Recently, two independent research groups reported on their studies on CeNiGe$_2$
single crystals [4–7]. Both teams confirmed the antiferromagnetic (AFM) ordering below
about 4 K and the spin reorientation at about 3 K. As might be expected from the uniaxial
character of the crystal structure of CeNiGe$_2$, the magnetic and transport properties have been
found to be strongly anisotropic. However, the two groups stated two different crystalline
directions for an antiferromagnetic easy axis, namely the unique $b$-axis was claimed in [4–
6] but the $c$-axis in [7]. It has to be stressed that in the two studies the descriptions of the
single-crystal morphology were the same, i.e. the crystals were thin plates perpendicular to
the $b$-axis.

The aim of this paper is to clarify the controversy and to complete the available data
set for single-crystalline CeNiGe$_2$. We report here the results of magnetic and electrical

---

[1] Author to whom any correspondence should be addressed.

transport measurements carried out along all three principal directions of the orthorhombic crystal structure of this compound.

## 2. Experimental details

Single crystals of $CeNiGe_2$ were grown by the flux method. First, a polycrystalline sample was synthesized from pure elements by arc melting in a titanium-gettered argon atmosphere. Next, the melted button was placed in an alumina crucible together with the appropriate amount of indium as a flux (Ce:In = 1:30). The crucible was sealed in an evacuated silica tube and heated up to 1175 °C. Subsequently the temperature was slowly (2–3 °C h$^{-1}$) reduced to 700 °C and then rapidly to 200 °C. Just afterwards the liquid flux was removed by decanting. Finally, the residual In film was etched away from crystalline facets in diluted $HNO_3$. The single crystals obtained had a metallic lustre and plate-like shape with a typical size of 2 mm × 3 mm and thickness of 0.5 mm. They were stable in air and against moisture.

A few well developed single crystals were oriented for physical measurements on a four-circle diffractometer, KUMA Diffraction KM-4. X-ray scans, carried out on each of the samples, showed that the naturally grown single-crystalline plates have their facets perpendicular to the principal directions of the orthorhombic crystal structure, with the shortest length being always along the $b$-axis (see the inset to figure 1(b)). The lattice parameters, determined from the single-crystal x-ray data, were $a = 4.241(3)$ Å, $b = 16.740(6)$ Å and $c = 4.196(3)$ Å, being thus in very good agreement with the previous results [1]. The chemical composition of the selected crystals was checked on a Phillips 515 scanning electron microscope equipped with an EDAX PV 9800 spectrometer. The EDX analysis yielded the composition (26% Ce, 23% Ni, 51% Ge), consistent with the formula $CeNiGe_2$.

The magnetic properties of single-crystalline $CeNiGe_2$ were studied in the temperature range 1.7–300 K and in magnetic fields up to 5 T, using a Quantum Design MPMS-5 SQUID magnetometer. The electrical resistivity and the magnetoresistivity were measured over the same temperature interval in magnetic fields up to 13 T, employing a conventional four-point DC technique. The Seebeck coefficient was measured in the range 5–300 K using a standard differential method with pure copper as a reference material.

## 3. Results and discussion

### 3.1. Magnetic properties

Figure 1(a) presents the temperature dependence of the inverse DC magnetic susceptibility of single-crystalline $CeNiGe_2$ measured in a magnetic field applied parallel to all three principal directions in the orthorhombic unit cell. Apparently, the susceptibility is strongly anisotropic over the whole temperature range studied. Above 120 K the $\chi^{-1}(T)$ curves follow a Curie–Weiss law with the following least-squares fitting parameters: $\mu_{eff} = 2.53\ \mu_B$ and $\theta_p = 23$ K for $B \parallel a$-axis; $\mu_{eff} = 2.57\ \mu_B$ and $\theta_p = -161$ K for $B \parallel b$-axis; and $\mu_{eff} = 2.64\ \mu_B$ and $\theta_p = -114$ K for $B \parallel c$-axis, where $\mu_{eff}$ is the effective magnetic moment and $\theta_p$ is the paramagnetic Curie temperature. In each case the values of $\mu_{eff}$ are close to the theoretical one calculated for a free $Ce^{3+}$ ion, thus indicating the presence of well localized cerium magnetic moments. Large differences between the $\theta_p$ values reflect the strong magnetocrystalline anisotropy.

As manifested by two distinct anomalies seen in figure 1(b) in the $\chi(T)$ curve measured for the $B \parallel a$-axis configuration in a field of 0.5 T, $CeNiGe_2$ orders antiferromagnetically at $T_N = 3.9$ K and then undergoes another phase transition at $T_1 = 3.2$ K, probably a change in the magnetic structure. As shown in figure 2(a), with increasing field strength the susceptibility
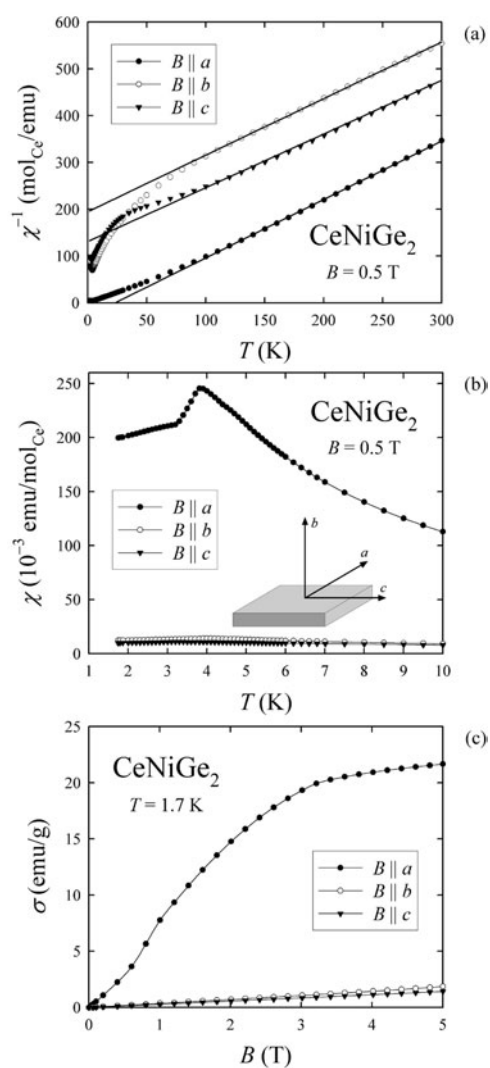
**Figure 1.** (a) The inverse DC magnetic susceptibility of CeNiGe$_2$ measured as a function of temperature in a field of 0.5 T. The solid lines are fits of the Curie–Weiss law to the experimental data. (b) $\chi(T)$ at low temperatures; the inset shows schematically the arrangement of the crystal axes in the crystals studied. (c) The field dependence of the magnetization of CeNiGe$_2$ taken at 1.7 K.

maximum at $T_N$ moves to lower temperatures, as expected for antiferromagnets, and for that reason the singularity at $T_1$ becomes obscured. In fields $B \geqslant 1$ T the maximum at $T_N$ transforms into a kink but the rapid suppression of the Néel temperature with rising field is continued. Finally, for $B \geqslant 3.5$ T the $\chi(T)$ curves measured for $B \parallel a$-axis are already featureless above 1.7 K.

Figures 2(b) and (c) display the low temperature behaviour of the magnetic susceptibility of CeNiGe$_2$ measured in several different magnetic fields applied parallel to the $b$- and $c$-axis, respectively. In the $B \parallel b$-axis configuration there occurs in $\chi(T)$ a maximum at $T_N$ and a change in slope at $T_1$, both being only slightly shifted to lower temperatures with increasing
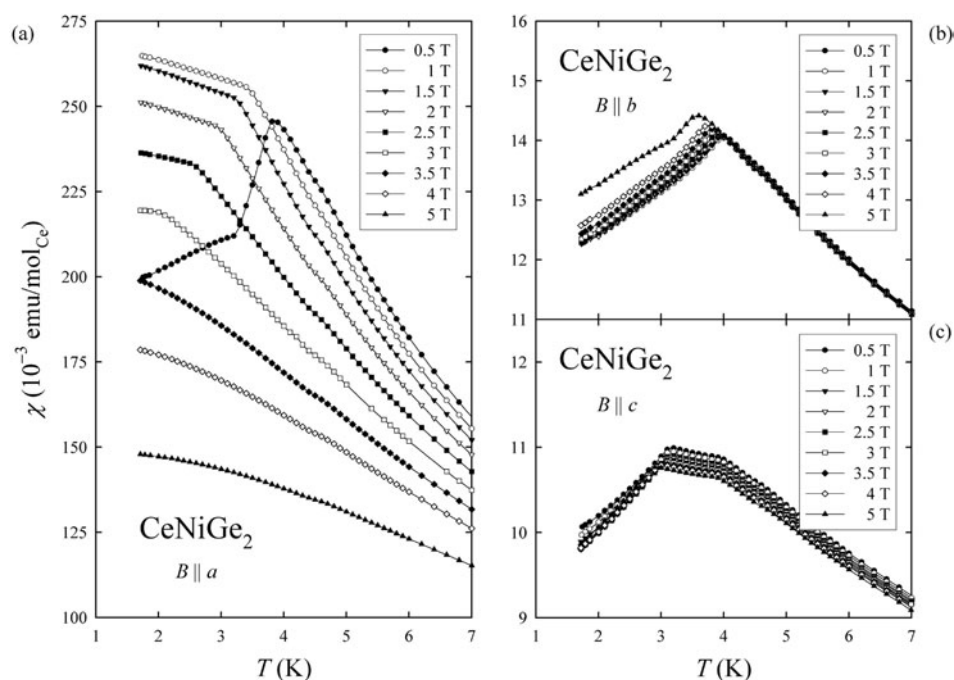
**Figure 2.** The temperature dependence of the DC magnetic susceptibility of CeNiGe$_2$ measured in several different magnetic fields applied parallel to the *a*-, *b*- and *c*-axes.

field. For the $B \parallel c$-axis case, the susceptibility exhibits two sharp kinks at $T_N$ and $T_1$. As is apparent from figure 2(c), the shapes of both anomalies are hardly affected by the magnetic field and the transition temperatures are only little suppressed with rising field. At this point it is also worth noting that for any field configuration and its strength no difference either in the magnitude of the magnetic susceptibility or in the shape of its temperature dependences was detected when performing the measurements upon cooling the sample in zero and finite magnetic fields.

A remarkable feature of the low temperature susceptibility of CeNiGe$_2$ is its huge anisotropy. As is evident from figure 1(b) and figures 2(a)–(c), the susceptibility measured for $B \parallel a$-axis is more than one order of magnitude stronger than the signals measured for $B \parallel b$-axis and $B \parallel c$-axis. This magnetic anisotropy manifests itself also in the field dependences of the magnetization of CeNiGe$_2$, displayed in figures 1(c), 3 and 4. The magnetization measured at 1.7 K along the *b*- and *c*-axes changes linearly with magnetic field nearly up to 5 T, and the same behaviour is observed at higher temperatures from the ordered region (see figure 4). For these two field configurations the values of the magnetization at each temperature are very similar, whereas those measured with $B \parallel a$-axis are an order of magnitude larger. The $\sigma(B)$ isotherms taken for the latter direction have more complex character (see figure 3(a)). At 1.7 K the magnetization is proportional to $B$ only up to about 0.5 T, and then $\sigma(B)$ shows a metamagnetic-like behaviour, thus corroborating an antiferromagnetic character of the low temperature ordering. In a field of about 3 T there occurs a less discernible anomaly in $\sigma(B)$ above which the magnetization bends for saturation in the strongest magnetic fields applied. At higher temperatures in the magnetically ordered region the low field metamagnetic transition is quite clearly seen but the other feature becomes nearly undetectable in $\sigma(B)$, yet still
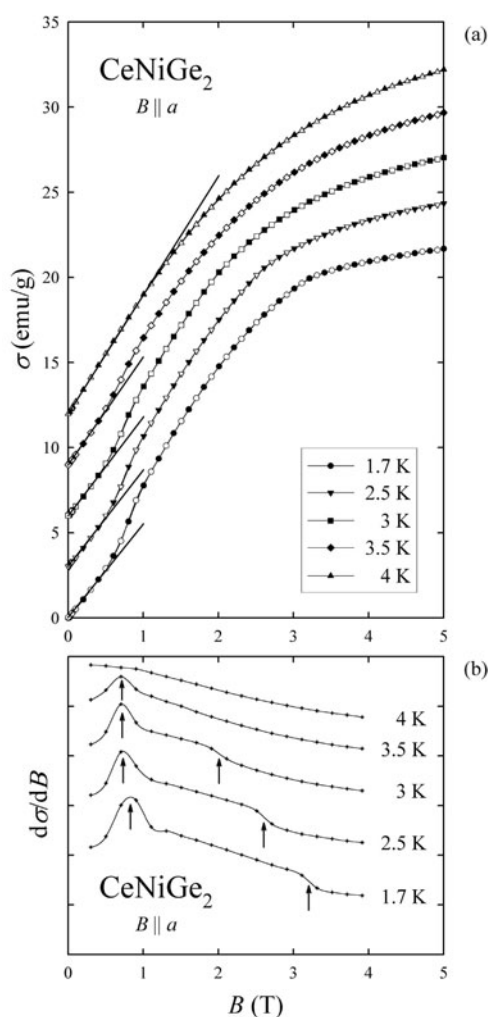
**Figure 3.** The field dependence of the magnetization of CeNiGe$_2$ measured at several different temperatures with increasing (closed symbols) and decreasing (open symbols) magnetic field applied along the $a$-axis. For the sake of clarity the $\sigma(B)$ curves are shifted upwards by amounts that are multiples of 3 emu g$^{-1}$. The straight solid lines emphasize the linear behaviour of the magnetization in weak fields. (b) The field derivative of the magnetization data from panel (a). The arrows mark the positions of metamagnetic transitions.

being observable in the field derivatives of the magnetization isotherms (note the arrows in figure 3(b)). Obviously, in the paramagnetic state (e.g. $T = 4$ K) neither of these two anomalies is present either in the $\sigma(B)$ or the d$\sigma$/d$B(B)$ curve.

### 3.2. Electrical transport properties

Figure 5(a) presents the temperature dependences of the electrical resistivity of a CeNiGe$_2$ single crystal measured in the absence of an external magnetic field with the electrical current flowing along the $a$- and $c$-axes. At room temperature the two resistivities have similar values and behave similarly with decreasing temperature down to about 100 K. Below this temperature
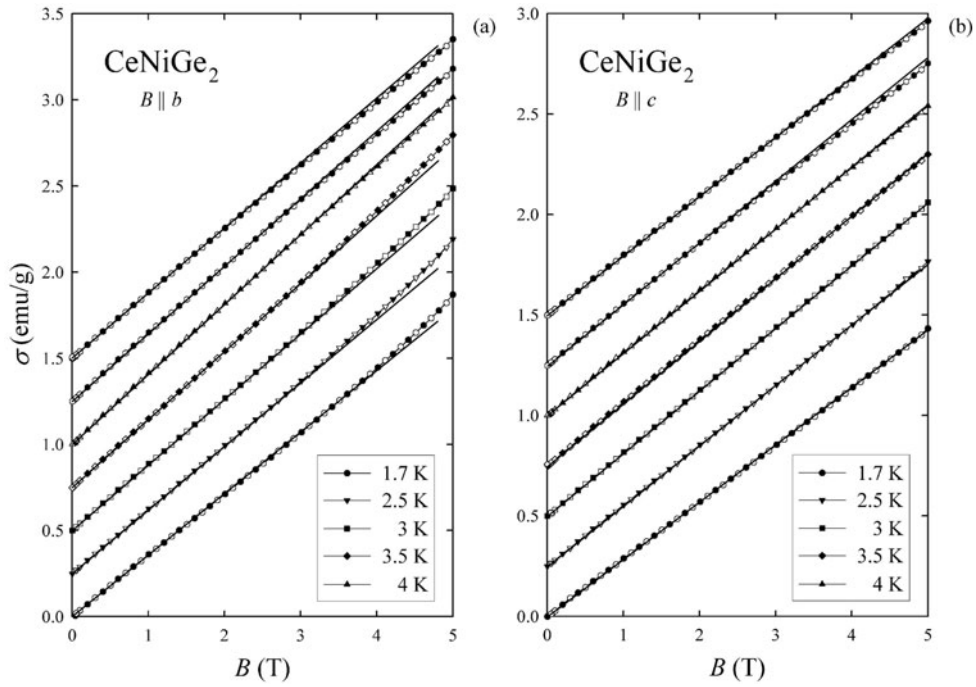
**Figure 4.** The field dependence of the magnetization of CeNiGe$_2$ measured at several different temperatures with increasing (closed symbols) and decreasing (open symbols) magnetic field applied parallel to the *b*- and *c*-axes. For the sake of clarity the $\sigma(B)$ curves are shifted upwards by amounts that are multiples of 0.25 emu g$^{-1}$. The straight solid lines emphasize the linear behaviour of the magnetization.

there appear considerable differences both in the shape and in the magnitude of $\rho(T)$. In the temperature range 70–300 K the resistivity measured for the $i \parallel a$ configuration is nearly temperature independent and $\rho(T)$ forms a weak broad maximum at about 90 K. At lower temperatures the resistivity develops first a minimum at about 20 K and then a maximum at about 5 K, i.e. slightly above $T_N$. In turn, the resistivity measured along the *c*-axis initially hardly changes with decreasing temperature from 300 K down to 100 K, then goes through a broad hump in the vicinity of 90 K, rapidly decreases down to 20 K and, below this temperature, forms a plateau. In both $\rho(T)$ curves the antiferromagnetic ordering manifests itself as a sudden drop of the resistivity below $T_N$ (see the inset to figure 5(a)). In contrast, the spin reorientation at $T_1$ hardly affects the resistivity measured in either direction.

The influence of the transverse ($B \perp i$) magnetic field on the electrical resistivity of CeNiGe$_2$ is displayed in figure 5(b) for the case $i \parallel a$-axis and $B \parallel c$-axis. Upon applying a field the resistivity rapidly decreases and already in a field of 3 T the maximum visible on the zero-field curve at about 5 K as well as the anomaly due to the antiferromagnetic ordering at $T_N = 3.9$ K are no longer discernible. Figure 6(a) shows the transverse magnetoresistivity of CeNiGe$_2$ measured in the paramagnetic region as a function of magnetic field for the current and field configurations as above. For all temperatures and magnetic fields studied, $\Delta\rho/\rho(0)$ has negative values, and at 5 K it attains in $B = 13$ T values as large as over $-80\%$. The overall shape of the temperature-dependent magnetoresistivity is of the single-ion Kondo type [8–10]. Indeed, in agreement with Schlottmann's theory, the $\Delta\rho/\rho(0)$ isotherms form a universal curve when plotted versus $B/(T+T^*)$, where $T^*$ is a scaling parameter (see figure 6(b)). In the case of
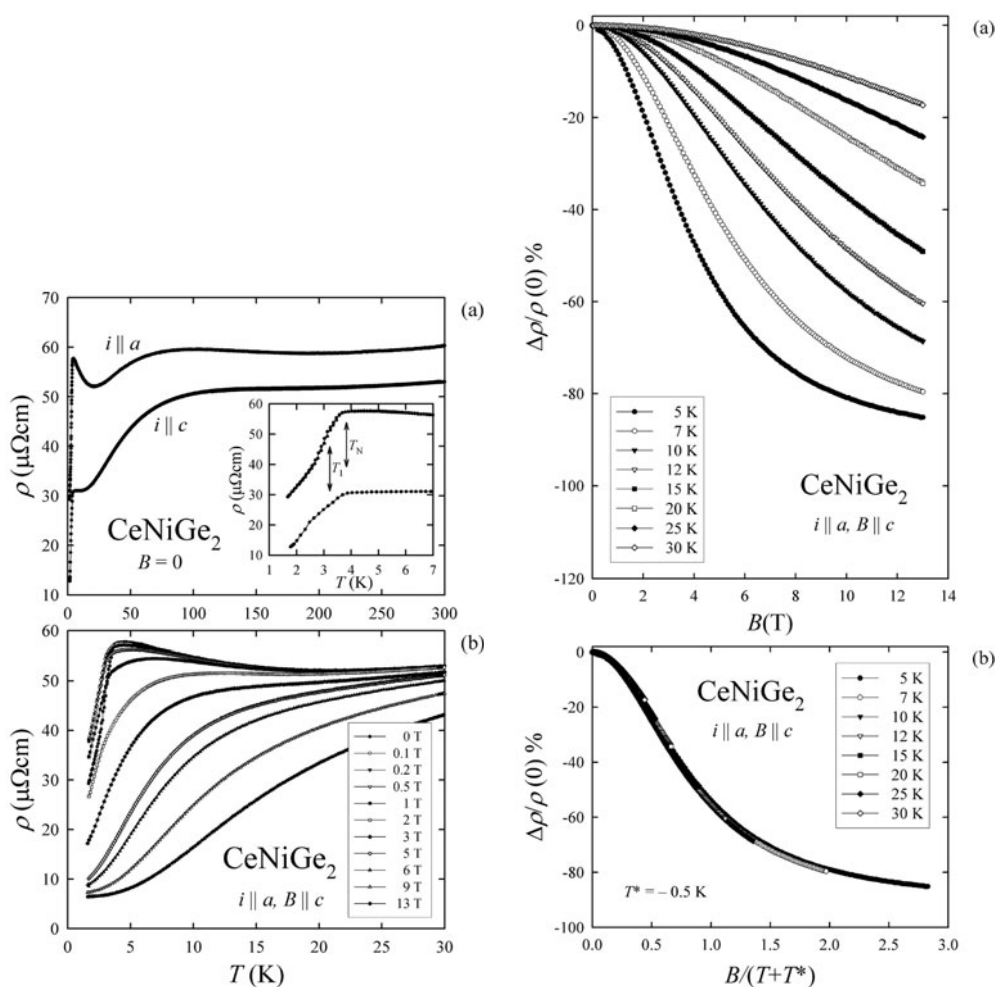
**Figure 5.** (a) The temperature dependence of the electrical resistivity of CeNiGe$_2$ measured along the $a$- and $c$-axes in zero magnetic field. The inset displays the resistivity in the vicinity of the magnetic phase transitions (marked by the arrows). (b) $\rho(T)$ taken along the $a$-axis in several different magnetic fields applied perpendicular to the $c$-axis.

**Figure 6.** (a) The transverse magnetoresistivity of CeNiGe$_2$ measured at several temperatures in the paramagnetic region with current flowing along the $a$-axis and magnetic field applied along the $c$-axis. (b) The single-ion Kondo scaling of the magnetoresistivity isotherms.

CeNiGe$_2$ the characteristic temperature is negative ($T^* = -0.5$ K), which implies the presence of strong correlations of ferromagnetic character, as observed e.g. in the heavy-fermion systems UBe$_{13}$, YbPtSn or CeNiGe$_3$ [11–13]. In figure 7 we show the transverse magnetoresistivity of CeNiGe$_2$ measured at several temperatures from the paramagnetic region in the configuration $i \parallel c$-axis and $B \parallel a$-axis. The magnetoresistivity measured in these latter conditions has absolute values approximately two orders of magnitude smaller than that previously discussed. Moreover, in contrast to the previous case it is negative only at 7 K, and positive at higher temperatures.

The temperature dependence of the thermoelectric power, measured along all three principal directions of single-crystalline CeNiGe$_2$, is presented in figure 8. In the temperature
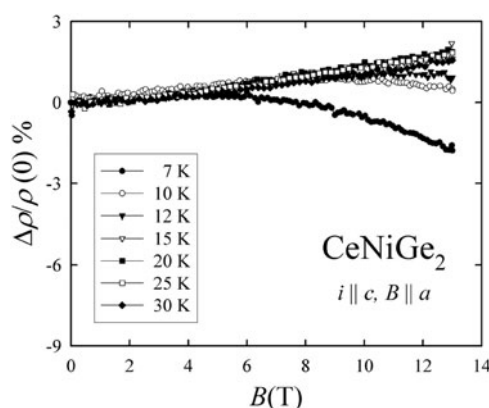
**Figure 7.** The transverse magnetoresistivity of CeNiGe$_2$ measured at several temperatures in the paramagnetic region with current flowing along the *c*-axis and magnetic field applied along the *a*-axis.
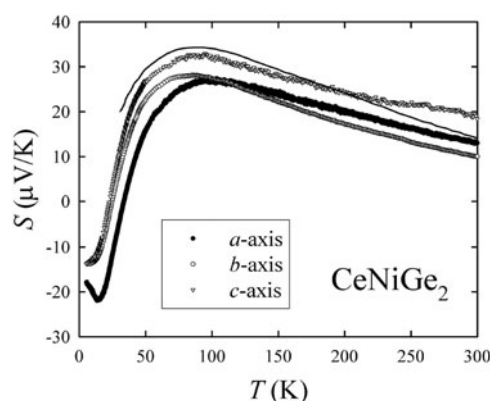
**Figure 8.** The temperature dependence of the Seebeck coefficient of CeNiGe$_2$ measured with the temperature gradient parallel to the *a*-, *b*- and *c*-axes. For comparison we show by the solid curve the $S(T)$ variation calculated for the Anderson lattice [14] with $T_0 = 100$ K; the theoretical $S$ values are arbitrarily divided here by 3.

range 30–300 K all the experimental curves have similar shapes, reasonably well approximated by the results of Anderson lattice calculations by Cox and Grewe [14] with the characteristic temperature $T_0$ of the order of 100 K (note the solid curve), which is consistent with the estimated crystal electric field (CEF) splitting in CeNiGe$_2$ [15]. At low temperatures the $S(T)$ curves measured for the temperature gradient applied along the *b*- and *c*-axes behave very similarly—the Seebeck coefficient changes sign from positive to negative near 30 K and then smoothly decreases down to 5 K. In contrast, $S(T)$ taken for the temperature gradient along the *a*-axis becomes negative at about 40 K and afterwards develops a distinct minimum at about 20 K.

## 4. Discussion

### 4.1. Characteristic temperatures

The results of magnetic and electrical measurements performed on single-crystalline CeNiGe$_2$ indicate that the compound studied is a Kondo antiferromagnet with strong CEF interactions. The AFM ordering clearly manifests itself in the temperature variations of both the magnetic susceptibility and the electrical resistivity in the form of characteristic anomalies occurring at $T_N = 3.9$ K. In turn, the subsequent spin structure rearrangement occurring at $T_1 = 3.2$ K brings about a distinct anomaly in the $\chi(T)$ curves, yet it hardly affects the resistivity. The magnitude of the CEF splitting may be estimated from the $\chi^{-1}(T)$ dependences, which become linear only above 100–120 K, thus suggesting that the $^2F_{5/2}$ ground multiplet of Ce$^{3+}$ ions is not totally populated below these temperatures. The total CEF splitting $\Delta \sim 100$ K is also consistent with the overall behaviour of the electrical resistivity and the thermoelectric power of CeNiGe$_2$. Both these characteristics show humps or maxima in their temperature variations at about 90–100 K, which—according to Cornut and Coqblin [16] and Cox and Grewe [14]—may be associated with the CEF effect. In turn, the minima visible at low temperatures in the $\rho(T)$ and $S(T)$ curves measured for the *a*-axis are characteristic of Kondo interactions, and allow one to estimate roughly the Kondo temperature, $T_K$, as being of the order of 20 K. Furthermore,

the presence of the Kondo-like interactions in CeNiGe$_2$ is confirmed by the behaviour of the magnetoresistivity isotherms taken in the paramagnetic region, which follow the single-ion Kondo scaling [8–10], as well as the temperature dependence of the Seebeck coefficient, which is characteristic for Kondo systems [14, 15]. Consequently, the formation of the low temperature maximum on the $\rho(T)$ curve that occurs in CeNiGe$_2$ at about 5 K (for $i \parallel a$-axis) should be associated with the coherence effect in the lattice of Kondo scattering centres.

For the most part the new results obtained in this work for CeNiGe$_2$ single crystals are in good agreement with the data reported before for polycrystalline samples. The antiferromagnetic character of the ordering of well localized magnetic moments of cerium ions with a two-step phase transition at low temperatures generally confirms the previous findings [2, 3], and even the previously reported ordering temperatures of about 4.0 and 3.2 K are in excellent agreement with $T_N$ and $T_1$ derived within the present studies. Moreover, in the $\rho(T)$ variations measured for polycrystals there were already discernible such features as the CEF maximum at $\approx 100$ K, the Kondo minimum at about 20 K and the coherence maximum at $\approx 6$ K [3]. More recent studies on single-crystalline CeNiGe$_2$ essentially corroborated the previous findings, especially those regarding two antiferromagnetic phase transitions at $T_N \approx 4$ K and $T_1 \approx 3$ K [4–7]. One should note, however, that in [4] the Kondo temperature was estimated to be about 45–50 K, and the total CEF splitting reported in [7] is as large as 653 K. Further studies, preferably direct determinations of these characteristic energy scales by means of inelastic neutron scattering, are required to solve the apparent discrepancies between the estimates given previously and in the present work.

When comparing the new results with the previously reported ones it is also worth noting that, in contrast to the magnetoresistivity data given in [4] for single-crystalline CeNiGe$_2$, which did not obey the single-ion Kondo scaling in any configuration of magnetic field and electrical current with respect to the crystallographic axes, in the present case the magnetoresistivity isotherms taken with $i \parallel a$-axis and $B \parallel c$-axis in the temperature range 5–30 K do follow the Schlottmann scaling, thus corroborating the Kondo character of the electrical transport in this compound.

## 4.2. Anisotropy axis

The strongly anisotropic properties of CeNiGe$_2$ were reported earlier for polycrystalline as well as single-crystalline samples [2, 4–6]. The authors of all these works have claimed a uniaxial anisotropy with the easy magnetization direction parallel to the crystallographic $b$-axis. Such anisotropy seems natural if one considers a quasi-tetragonal crystal structure of the compound with the unit cell strongly elongated along the $b$-axis (the ratios $b/a \approx b/c$ are about 4). Therefore, the most unexpected result obtained in the present study is that the unique magnetic direction in CeNiGe$_2$ is not the $b$-axis but the $a$-axis.

One should stress that this statement which contradicts the previous findings is firmly based on detailed investigations carried out on several single crystals of CeNiGe$_2$, which were oriented for physical studies by means of x-ray methods. In general, the shapes of the $\chi(T)$ and $\sigma(B)$ curves as well as the absolute values of the susceptibility and magnetization found are almost identical to those presented in [4–6] for single-crystalline specimens, yet the assignment of the crystallographic axes in this work is apparently different from the previous one. Interestingly, the $\chi(T)$ curve reported in [2] for a polycrystalline specimen exhibits a shape very similar to that found in the present work just for the configuration $B \parallel a$-axis. It is remarkable that at low temperatures the values of the magnetic susceptibility and the magnetization measured with the magnetic field parallel to the $a$-axis are here over one order of magnitude higher than those taken for the configuration $B \perp a$-axis. Another interesting

finding is that the overall temperature variation of the electrical resistivity of polycrystalline material [3] closely resembles the $\rho(T)$ curve measured in this work for a single crystal for the current flowing along the $a$-axis. From these comparisons it seems likely that the polycrystalline samples investigated in [2] and [3] were strongly textured, with the $a$-axis being the preferred orientation of grains. Finally, in the context of the easy axis assignment it is worth noting that the magnetoresistivity data on CeNiGe$_2$ show a clear Kondo-like character only for the $i \parallel a$-axis, and the temperature-dependent thermopower exhibits a Kondo-like minimum only when measured with the temperature gradient parallel to the $a$-axis.

## 5. Summary

The compound CeNiGe$_2$ is an antiferromagnetically ordered dense Kondo system with rather complex magnetic behaviour at low temperatures and a strong crystalline electric field effect. The characteristic temperatures associated with the CEF interactions, the Kondo scattering and the AFM ordering phenomena are about 100, 20 and 4 K, respectively. The magnetic and electrical transport properties of CeNiGe$_2$ are strongly anisotropic over the whole temperature range investigated, with the $a$-axis being the unique direction. This latter finding contradicts the previous studies [2, 4–6] which all have claimed uniaxial anisotropy along the $b$-axis. Most interestingly, the new description is in line with the most recent paper by Okada *et al* [7] who state that all the previous reports on CeNiGe$_2$ were mistaken as regards the directions of the crystals studied. It must be noted, however, that the easy magnetization direction given in [7] is the $c$-axis; i.e. for some unclear reasons it is also different from the result obtained in the present work. Further experiments concerning the magnetic structure of CeNiGe$_2$, e.g. neutron scattering ones, are needed to clarify the controversies on the easy axis in the compound.

## Acknowledgments

## References

[1] Bodak O I and Gladyshevskii E I 1969 *Kristallografiya* **14** 990
[2] Pecharsky V K, Gschneidner K A and Miller L L 1991 *Phys. Rev.* B **43** 10906
[3] Geibel C, Kämmerer C, Seidel B, Bredl C D, Grauel A and Steglich F 1992 *J. Magn. Magn. Mater.* **108** 207
[4] Jung M H, Harrison N, Lacerda A H, Nakotte H, Pagliuso P G, Sarrao J L and Thompson J D 2002 *Phys. Rev.* B **66** 054420
[5] Jung M H, Lacerda A H, Pagliuso P G, Sarrao J L and Thompson J D 2002 *J. Appl. Phys.* **91** 8522
[6] Alsmadi A M, Nakotte H, Sarrao J L, Jung M H and Lacerda A H 2003 *J. Appl. Phys.* **93** 8343
[7] Okada Y, Inada Y, Galatanu A, Yamamoto E, Settai R and Ōnuki Y 2003 *J. Phys. Soc. Japan* **72** 2692
[8] Schlottmann P 1987 *Phys. Rev.* B **35** 5279
[9] Schlottmann P 1989 *Phys. Rep.* **181** 1
[10] Batlogg B, Bishop D J, Bucher E, Golding J G, Ramirez A P, Fisk Z, Smith J L and Ott H R 1987 *J. Magn. Magn. Mater.* **63/64** 441
[11] Andraka B and Stewart G R 1994 *Phys. Rev.* B **49** 12359
[12] Pietri R, Andraka B, Kaczorowski D, Leithe-Jasper A and Rogl P 2000 *Phys. Rev.* B **61** 12169
[13] Pikul A P, Kaczorowski D, Plackowski T, Czopnik A, Michor H, Bauer E, Hilscher G, Rogl P and Grin Yu 2003 *Phys. Rev.* B **67** 224417
[14] Cox D L and Grewe N 1988 *Z. Phys.* B **71** 321
[15] Bhattacharjee A K and Coqblin B 1976 *Phys. Rev.* B **13** 3441
[16] Cornut D and Coqblin B 1972 *Phys. Rev.* B **5** 4541